Slow Passage Through Resonance in Mathieu's Equation

LESLIE NG
RICHARD RAND
MICHAEL O'NEIL
Department of Theoretical and Applied Mechanics, Cornell University, Ithaca, NY 14853, USA

(Received 5 November 2001; accepted 29 May 2002)

Abstract: We investigate slow passage through the 2:1 resonance tongue in Mathieu's equation. Using numerical integration, we find that amplification or de-amplification can occur. The amount of amplification (or de-amplification) depends on the speed of travel through the tongue and the initial conditions. We use the method of multiple scales to obtain a slow flow approximation. The Wentzel–Kramers–Brillouin (WKB) method is then applied to the slow flow equations to obtain an analytic approximation.

Key Words: Resonance, Mathieu equation, amplification, parametric excitation

1. INTRODUCTION

Mathieu's equation is the following second-order linear non-autonomous ordinary differential equation (ODE):

$$\frac{\mathrm{d}^2x}{\mathrm{d}t^2} + (\delta + \epsilon\cos t)x = 0. \tag{1}$$

Equation (1) has been widely studied (Stoker, 1950). For given values of the parameters δ and ϵ, either all the solutions are bounded (stable) or an unbounded solution exists (unstable). Figure 1 shows the transition curves separating regions of instability from those of stability for equation (1) in the δ–ϵ parameter plane. These regions of instability are commonly referred to as resonance tongues.

In this paper, we investigate what happens if δ changes slowly in time. In particular, we assume δ varies linearly with time and we replace δ in equation (1) with

$$\delta = \sigma + \epsilon^2\mu t. \tag{2}$$

For fixed values of ϵ, we can think of a point (δ, ϵ) moving in time across the δ–ϵ plane in and out of the tongues of instability. The constant term σ is the initial value of δ at time $t = 0$ and $\epsilon^2\mu$ is the speed at which the point (δ, ϵ) moves across the δ–ϵ plane. Putting equation (2) into equation (1) results in the following ODE

Journal of Vibration and Control, **9**: 685–707, 2003
DOI: 10.1177/107754603029581

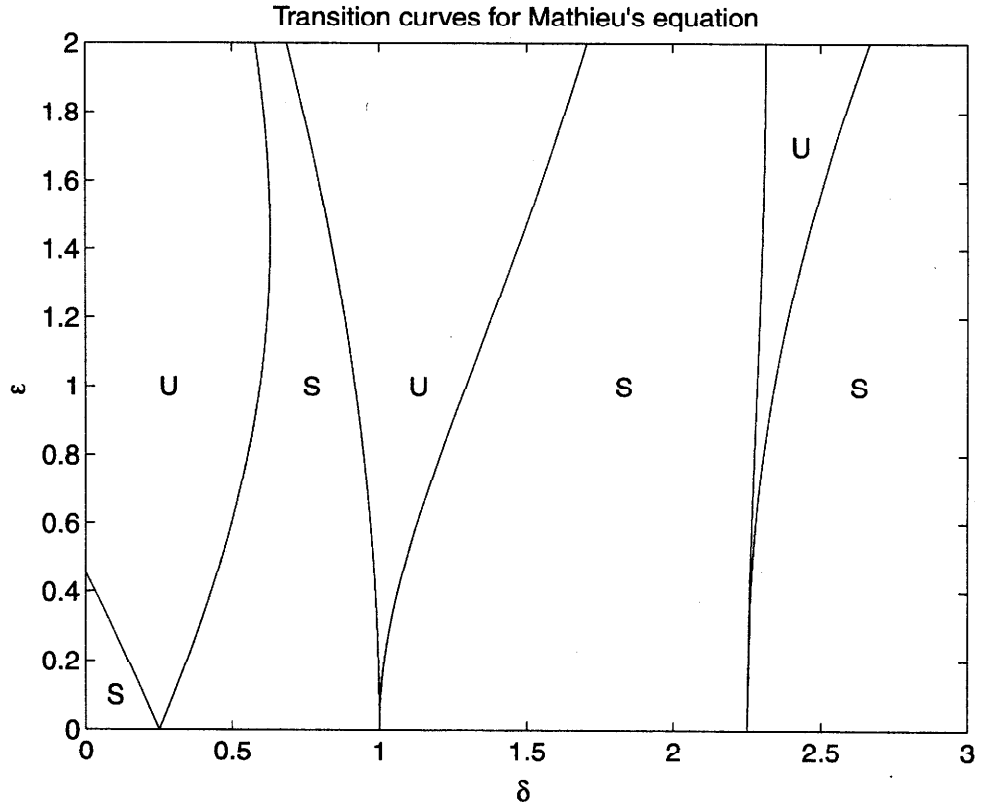

Figure 1. Regions of stability and instability in Mathieu's equation (S denotes stable and U denotes unstable).

$$\frac{\mathrm{d}^2x}{\mathrm{d}t^2} + (\sigma + \epsilon^2\mu t + \epsilon\cos t)x = 0 \tag{3}$$

which we study using numerical integration and perturbation methods for small values of ϵ.

In previous work, Nayfeh and Asfar (1988) and Neal and Nayfeh (1990) have investigated slow passage through resonance in Mathieu's equation with additional cubic and damping terms. After using the method of multiple scales to derive a slow flow, they have performed a numerical investigation of the slow flow and reported on the different phenomena observed.

Raman et al. (1996) have presented a general methodology for analyzing slow passage across instabilities in nonlinear dissipative systems. They presented some analytic results for the system studied by Nayfeh and Asfar. In a second paper, Raman and Bajaj (1998) have presented some general results for Hamiltonian oscillators. As an example, they investigated slow passage through resonance in Mathieu's equation with an additional cubic nonlinearity.

The above-mentioned studies all look at variations of the Mathieu equation with a nonlinear term. The effect of the nonlinearity is to include stable nontrivial solutions in the resonance tongue as opposed to just having an unbounded solution in the case of the

linear Mathieu equation. The analysis focuses on the transition from the trivial solution to the bifurcating solution while going through the resonance tongue.

In a related work, Lebovitz and Pesci (1995) have treated separatrix crossing in nonlinear Hamiltonian systems which possess a slowly varying homoclinic loop. They characterized certain solutions which approach the unstable equilibrium on a $1/\epsilon$ timescale, so-called "hovering" solutions. In contrast to their work, in the present paper we are concerned with a linear Hamiltonian system in which the Hamiltonian depends on both t and ϵt (regular time and slow time), and the slowly-varying unstable eigenspace exists for a finite time.

In contrast to these works, in this paper we focus on passage through resonance in the linear Mathieu equation and the question of amplification, which is described in the next section.

2. NUMERICAL INTEGRATION

We begin our study by numerically integrating equation (3) to get an idea of what occurs when crossing a resonance tongue of Mathieu's equation. The 2:1 resonance in Mathieu's equation is the most prominent so we choose parameter values and initial conditions that correspond to transversing the 2:1 resonance tongue from left to right in the δ–ϵ plane for a fixed value of ϵ.

For small values of ϵ, the first term approximation of the transition curves of the 2:1 resonance tongue in Mathieu's equation is

$$\delta = \frac{1}{4} \pm \frac{\epsilon}{2} + O(\epsilon^2), \qquad \epsilon \ll 1. \tag{4}$$

The minus sign corresponds to the left transition curve and the plus sign corresponds to the right transition curve. Replacing δ in equation (4) with equation (2) we have

$$\sigma + \epsilon^2 \mu t \approx \frac{1}{4} \pm \frac{\epsilon}{2}. \tag{5}$$

From equation (5), we can solve for the times that would correspond to being on the left transition curve t_- and on the right transition curve t_+:

$$t_- \approx \frac{1 - 4\sigma}{4\epsilon^2 \mu} - \frac{1}{2\epsilon\mu}, \qquad t_+ \approx \frac{1 - 4\sigma}{4\epsilon^2 \mu} + \frac{1}{2\epsilon\mu}. \tag{6}$$

For our numerical integrations, we choose the initial condition such that

$$x(t_0) = \cos\gamma, \qquad \frac{\mathrm{d}x}{\mathrm{d}t}(t_0) = \sin\gamma \tag{7}$$

where $0 \leq \gamma < 2\pi$.

Figure 2 shows a numerical integration for $\epsilon = 0.1, \mu = 0.1, \sigma = 0, t_0 = 0$ and $\gamma = 0$. Also shown by dashed lines are the times that correspond to being on the transition curves ($t_- = 200$ and $t_+ = 300$).

Figure 3 shows a numerical integration with the same parameter values as in Figure 2 but with different initial conditions ($\gamma = \pi/2$). Comparing Figures 2 and 3, we see that they

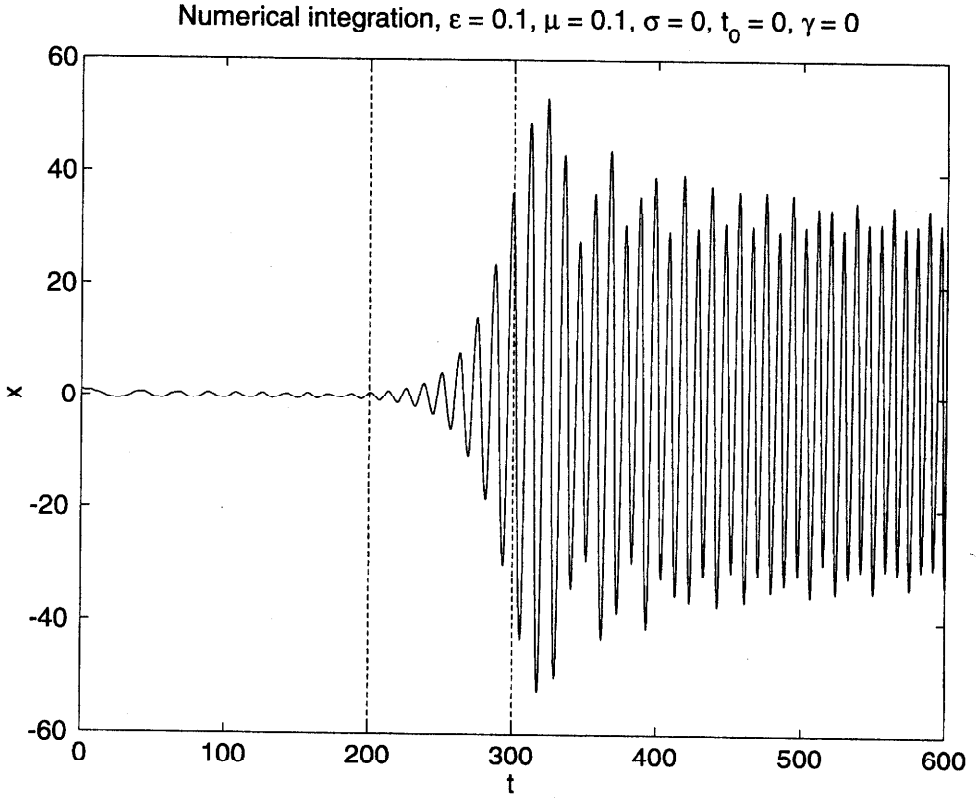

Figure 2. Numerical integration of equation (3) for $\gamma = 0$, i.e. for $x(0) = 1$, $\frac{dx}{dt} = 0$. Note that the vertical axis is scaled to a maximum of 60. The parameters are $\epsilon = 0.1$, $\mu = 0.1$ and $\sigma = 0$. The dashed vertical lines show approximate times at which the motion crosses the transition curves in the Mathieu equation (1): $t_- = 200$ and $t_+ = 300$.

both exhibit amplification as a result of going through the resonance tongue, although the maximum amplitude in Figure 3 is considerably larger than that in Figure 2. Also note that in both Figures 2 and 3, the maximum amplitude occurs at the time which is larger than t_+, that is, after the motion has exited the resonance tongue.

To investigate the effects of the initial conditions on amplification, we numerically integrate equation (3) for the same parameter values using a range of initial conditions ($0 \leq \gamma < 2\pi$). Figure 4 shows a plot of the maximum value of x as a function of the initial condition parameter γ. We see that the amplification can vary significantly depending on the initial conditions. Figure 5 shows a numerical integration for the initial condition $\gamma = 2.9558$ that is approximately the value of γ which has the least amplification in Figure 4. For $\gamma = 2.9558$ we see that the maximum amplitude is smaller after going through the tongue than it was prior to entering the tongue. We find that a small range of initial conditions results in de-amplification after going through the resonance tongue.

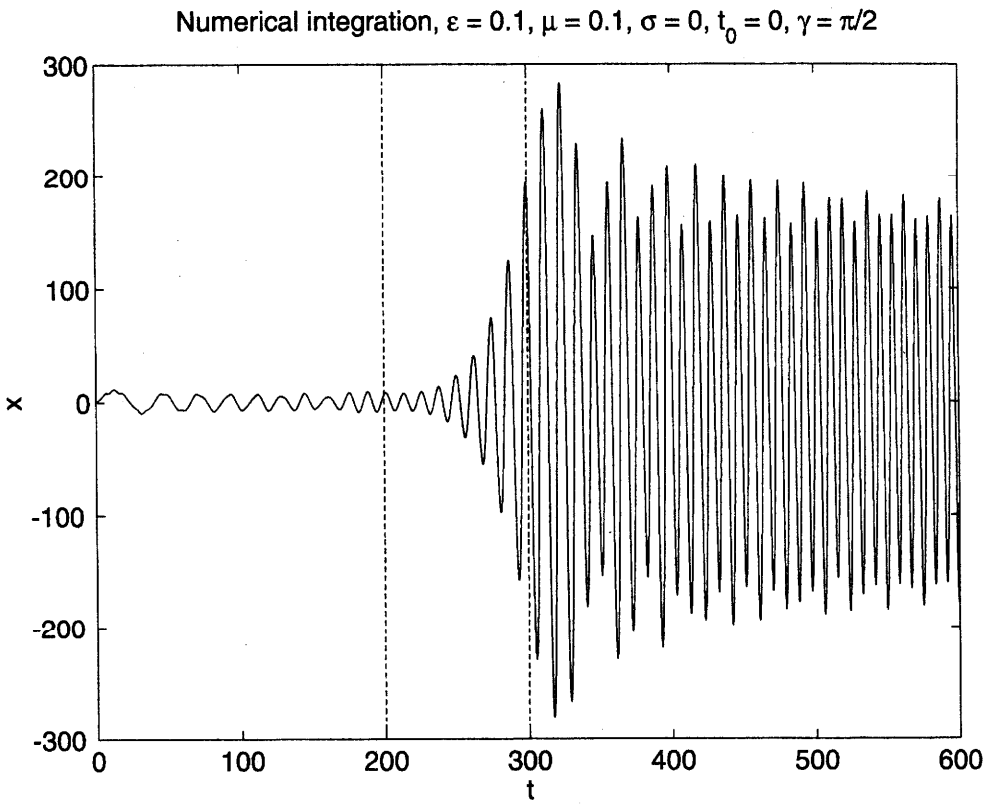

Figure 3. Numerical integration of equation (3) for $\gamma = \frac{\pi}{2}$, i.e. for $x(0) = 0$, $\frac{dx}{dt} = 1$. Note that the vertical axis is scaled to a maximum of 300. The parameters are $\epsilon = 0.1$, $\mu = 0.1$ and $\sigma = 0$. The dashed vertical lines show approximate times at which the motion crosses the transition curves in the Mathieu equation (1): $t_- = 200$ and $t_+ = 300$.

3. SLOW FLOW EQUATIONS

We use the method of multiple scales (Holmes, 1995; Bender and Orszag, 1999) to obtain an analytic approximation for equation (3) around the 2:1 resonance tongue ($\sigma = 1/4$) for $\epsilon \ll 1$. Here we set $\sigma = 1/4$ so that at $t = 0$ we are located exactly at the 2:1 resonance $\delta = 1/4$, i.e. in the middle of the associated tongue of instability. We start by introducing slow and fast time variables $\eta = \epsilon t$ and $\xi = t$. Equation (3) becomes

$$\frac{\partial^2 x}{\partial \xi^2} + 2\epsilon \frac{\partial^2 x}{\partial \xi \partial \eta} + \epsilon^2 \frac{\partial^2 x}{\partial^2 \eta} + \left(\frac{1}{4} + \epsilon\mu\eta + \epsilon \cos\xi\right) x = 0. \tag{8}$$

Taking $x(\xi, \eta)$ as a power series $x(\xi, \eta) = x_0(\xi, \eta) + \epsilon x_1(\xi, \eta) + \ldots$ and collecting $O(1)$ and $O(\epsilon)$ terms gives

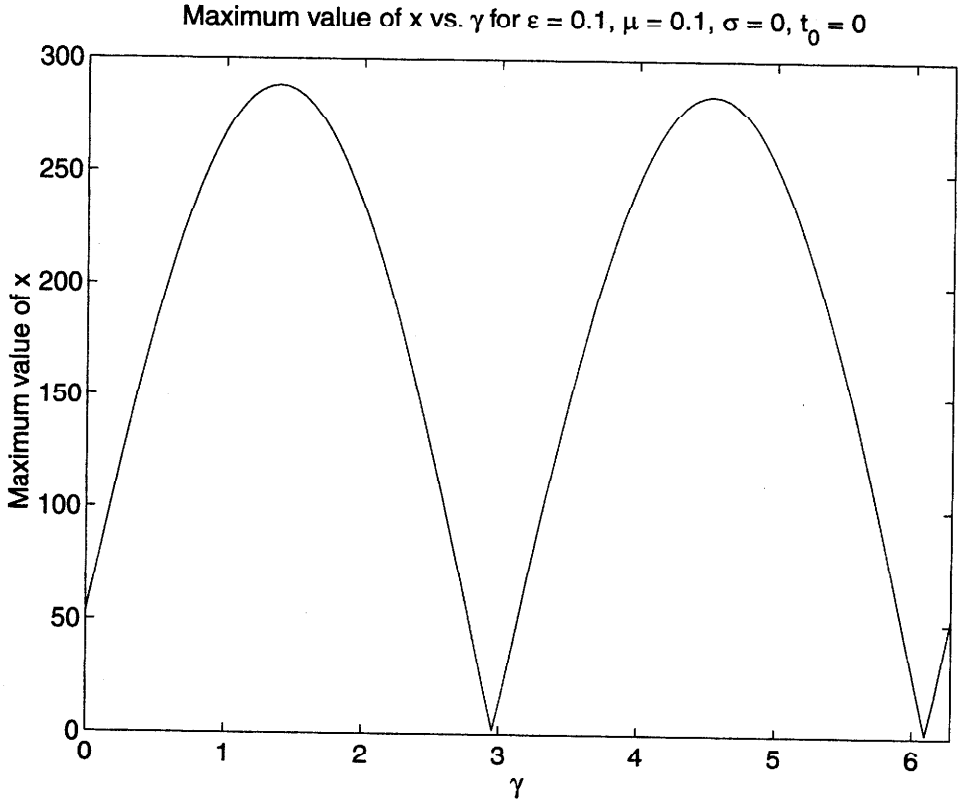

Figure 4. Maximum value of x as a function of the initial condition parameter γ where γ is defined in equation (7). The parameters are $\epsilon = 0.1$, $\mu = 0.1$ and $\sigma = 0$.

$$O(1) \quad : \quad \frac{\partial^2 x_0}{\partial \xi^2} + \frac{1}{4} x_0 = 0 \tag{9}$$

$$O(\epsilon) \quad : \quad \frac{\partial^2 x_1}{\partial \xi^2} + \frac{1}{4} x_1 = -2 \frac{\partial^2 x_0}{\partial \xi \partial \eta} - x_0 \cos \xi - \mu \eta x_0. \tag{10}$$

The general solution of equation (9) is

$$x_0(\xi, \eta) = A(\eta) \cos \frac{\xi}{2} + B(\eta) \sin \frac{\xi}{2}. \tag{11}$$

Substituting equation (11) into equation (10) and simplifying trigonometric terms gives

$$\begin{aligned} \frac{\partial^2 x_1}{\partial \xi^2} + \frac{1}{4} x_1 &= \left(\frac{\mathrm{d}A}{\mathrm{d}\eta} - \mu \eta B \right) \sin \frac{\xi}{2} - \left(\frac{\mathrm{d}B}{\mathrm{d}\eta} + \mu \eta A \right) \cos \frac{\xi}{2} \\ &- \frac{A}{2} \left(\cos \frac{3\xi}{2} + \cos \frac{\xi}{2} \right) - \frac{B}{2} \left(\sin \frac{3\xi}{2} - \sin \frac{\xi}{2} \right). \end{aligned} \tag{12}$$

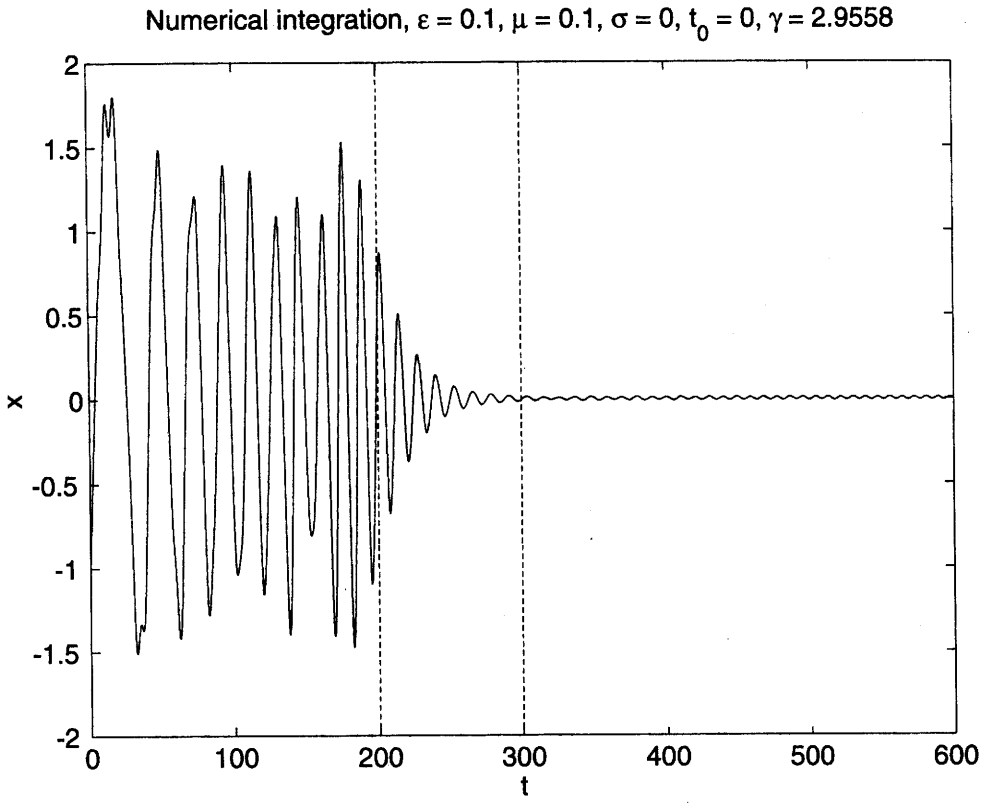

Figure 5. Numerical integration of equation (3) for $\gamma = 2.9558$. Note that the vertical axis is scaled to a maximum of 2. The parameters are $\epsilon = 0.1$, $\mu = 0.1$ and $\sigma = 0$. The dashed vertical lines show approximate times at which the motion crosses the transition curves in the Mathieu equation (1): $t_- = 200$ and $t_+ = 300$.

The removal of secular terms results in the slow flow equations:

$$\frac{dA}{d\eta} = \left(\mu\eta - \frac{1}{2}\right) B \tag{13}$$

$$\frac{dB}{d\eta} = -\left(\mu\eta + \frac{1}{2}\right) A. \tag{14}$$

Equations (13) and (14) can be combined to form a single second-order ODE in either A or B alone. Taking the derivative of equation (13) with respect to η gives

$$\frac{d^2A}{d\eta^2} = \left(\mu\eta - \frac{1}{2}\right) \frac{dB}{d\eta} + \mu B. \tag{15}$$

Substituting equations (13) and (14) into equation (15) gives the following second-order ODE in A alone

$$\frac{\mathrm{d}^2A}{\mathrm{d}\eta^2} = -\left(\mu\eta - \frac{1}{2}\right)\left(\mu\eta + \frac{1}{2}\right)A + \frac{\mu}{\mu\eta - \frac{1}{2}}\frac{\mathrm{d}A}{\mathrm{d}\eta}. \tag{16}$$

Setting $\tau = \mu\eta$, equation (16) can be rewritten as

$$\mu^2\frac{\mathrm{d}^2A}{\mathrm{d}\tau^2} + \left(\tau^2 - \frac{1}{4}\right)A - \frac{\mu^2}{\tau - \frac{1}{2}}\frac{\mathrm{d}A}{\mathrm{d}\tau} = 0. \tag{17}$$

Applying the same procedure but eliminating A gives the ODE in B:

$$\mu^2\frac{\mathrm{d}^2B}{\mathrm{d}\tau^2} + \left(\tau^2 - \frac{1}{4}\right)B - \frac{\mu^2}{\tau + \frac{1}{2}}\frac{\mathrm{d}B}{\mathrm{d}\tau} = 0. \tag{18}$$

Note that equation (17) is singular when $\tau = 1/2$ and equation (18) is singular when $\tau = -1/2$.

To compare the multiple scales approximation with the original equation using numerical integration, we need to relate the initial conditions of the original equation to the initial conditions of the slow flow equations. From equation (11), the multiple scales approximation to first order is

$$x(t) \sim A(\eta)\cos\frac{\xi}{2} + B(\eta)\sin\frac{\xi}{2} = A(\epsilon t)\cos\frac{t}{2} + B(\epsilon t)\sin\frac{t}{2}. \tag{19}$$

Taking the derivative with respect to time of equation (19), we obtain

$$\frac{\mathrm{d}x(t)}{\mathrm{d}t} \sim \epsilon A'(\epsilon t)\cos\frac{t}{2} - \frac{A(\epsilon t)}{2}\sin\frac{t}{2} + \epsilon B'(\epsilon t)\sin\frac{t}{2} + \frac{B(\epsilon t)}{2}\cos\frac{t}{2}. \tag{20}$$

Using equations (13) and (14) for $A'(\eta)$ and $B'(\eta)$, equation (20) can be written as

$$\frac{\mathrm{d}x(t)}{\mathrm{d}t} \sim \left(\epsilon\left(\mu\epsilon t - \frac{1}{2}\right) + \frac{1}{2}\right)B(\epsilon t)\cos\frac{t}{2} + \left(-\epsilon\left(\mu\epsilon t + \frac{1}{2}\right) - \frac{1}{2}\right)A(\epsilon t)\sin\frac{t}{2}. \tag{21}$$

At a time $t = t_0$, given $A(\eta_0)$ and $B(\eta_0)$ (where $\eta_0 = \epsilon t_0$) we can solve for the initial conditions $x(t_0)$ and $\frac{\mathrm{d}x}{\mathrm{d}t}(t_0)$ using equations (19) and (21). Figure 6 shows a comparison of the multiple scales approximation with the original equation, both obtained by numerical integration, for $\epsilon = 0.1, \mu = 0.1$ and $\sigma = 1/4$, with initial conditions $t_0 = -100, A(\eta_0) = 1$ and $B(\eta_0) = 0$. Note that the numerical integrations displayed in Figures 2, 3 and 5 used $\sigma = 0$ and $t_0 = 0$, so that the initial time in those figures corresponds to $t_0 = -250$.

We can see in Figure 6 that the multiple scales solution is a good approximation to the original equation until about the middle of the resonance tongue ($t \approx 0$). As the approximation worsens, the phase is still well approximated but the amplitude is slightly larger. At around $t \approx 150$, the phase starts to deviate as well. We also find that, if we

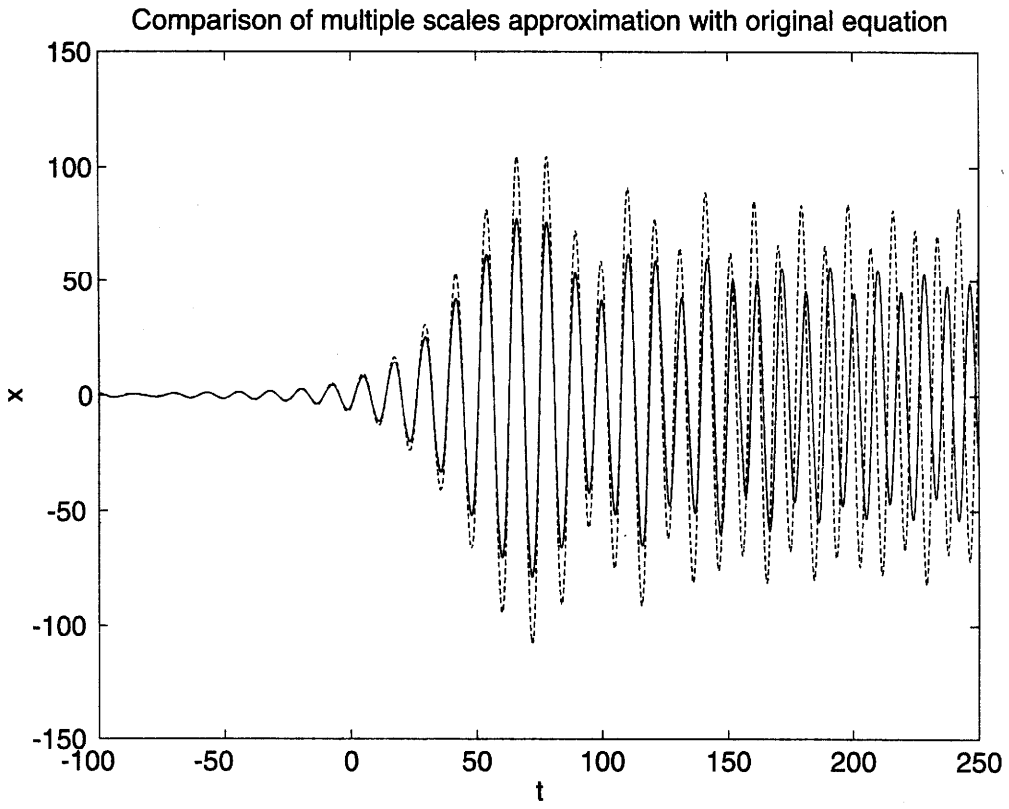

Figure 6. Comparison of the multiple scales approximation with the original equation. The solid line denotes the original equation, and the dashed line denotes the multiple scales approximation. The parameters are $\epsilon = 0.1$, $\mu = 0.1$ and $\sigma = 1/4$. The initial conditions are $A(\eta_0) = 1$, $B(\eta_0) = 0$, $\eta_0 = \epsilon t_0$, and $t_0 = -100$.

decrease the value of t_0 so the initial conditions are farther away from the tongue, the entire approximation becomes worse. This is because we are perturbing off the 2:1 resonance at $t = 0$. As $|t|$ increases, we become farther away from the 2:1 resonance and the approximation is no longer valid.

To investigate the effects of varying initial conditions, we assume the initial conditions are of the form

$$A(\eta_0) = \cos\kappa, \qquad B(\eta_0) = \sin\kappa \tag{22}$$

where $0 \leq \kappa < 2\pi$. We choose to vary the initial conditions now using κ instead of γ (equation (7)) because it restricts $A(\eta_0)^2 + B(\eta_0)^2 = 1$. Using γ restricts $x(t_0)^2 + \frac{dx}{dt}(t_0)^2 = 1$.

As in Figure 4, we numerically integrate the original equation and the multiple scales approximation for a range of initial conditions. Figure 7 shows the maximum value of x for the multiple scales approximation and the original equation as a function of the initial

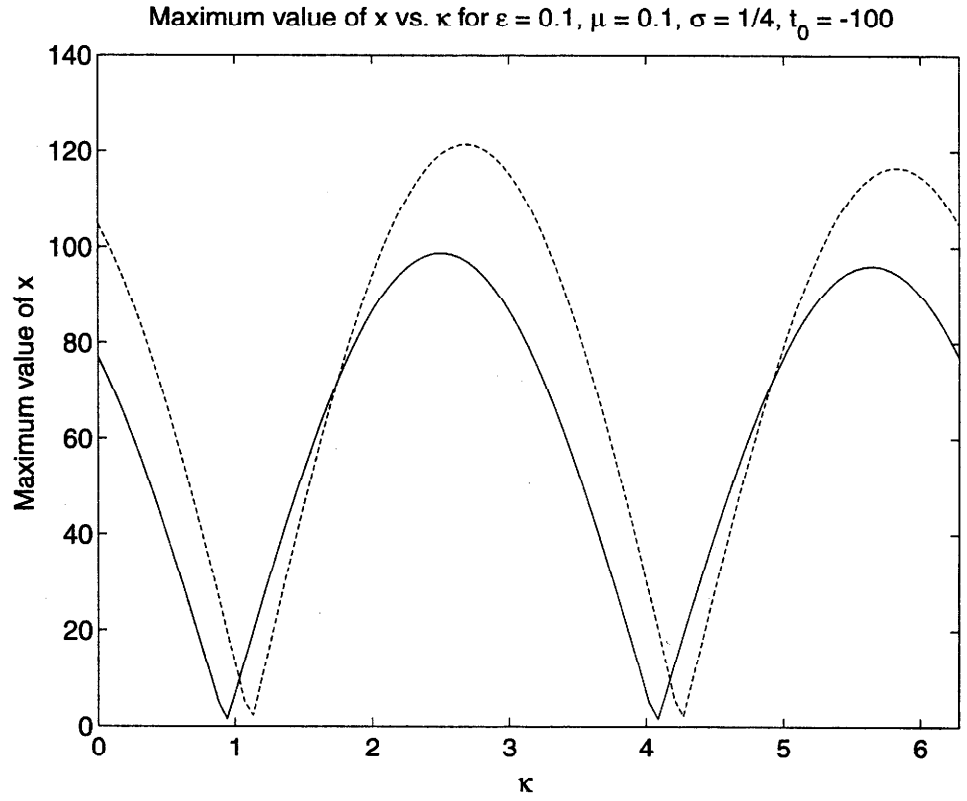

Figure 7. Comparison of the multiple scales approximation with the original equation. The solid line denotes the original equation, and the dashed line denotes the multiple scales approximation. The maximum value of x is shown as a function of the initial condition parameter κ for $t_0 = -100$.

condition parameter κ for $t_0 = -100$. We see that the multiple scales approximation predicts larger values but the dependence as a function of κ is still close.

Figure 8 shows a similar plot but for $t_0 = 0$. Again, the multiple scales approximation is still larger but the dependence on κ is closer. As expected, the initial conditions starting closer to $t_0 = 0$ give better approximations.

4. WENTZEL–KRAMERS–BRILLOUIN APPROXIMATION

4.1. Description of the Method

The Wentzel–Kramers–Brillouin (WKB) method (Holmes, 1995; Bender and Orszag, 1999) can be applied to linear ODEs where the highest derivative is multiplied by a small perturbation parameter. Equations (17) and (18) are of the form

$$\mu^2 y'' - q(\tau)y + \mu^2 p(\tau)y' = 0 \tag{23}$$

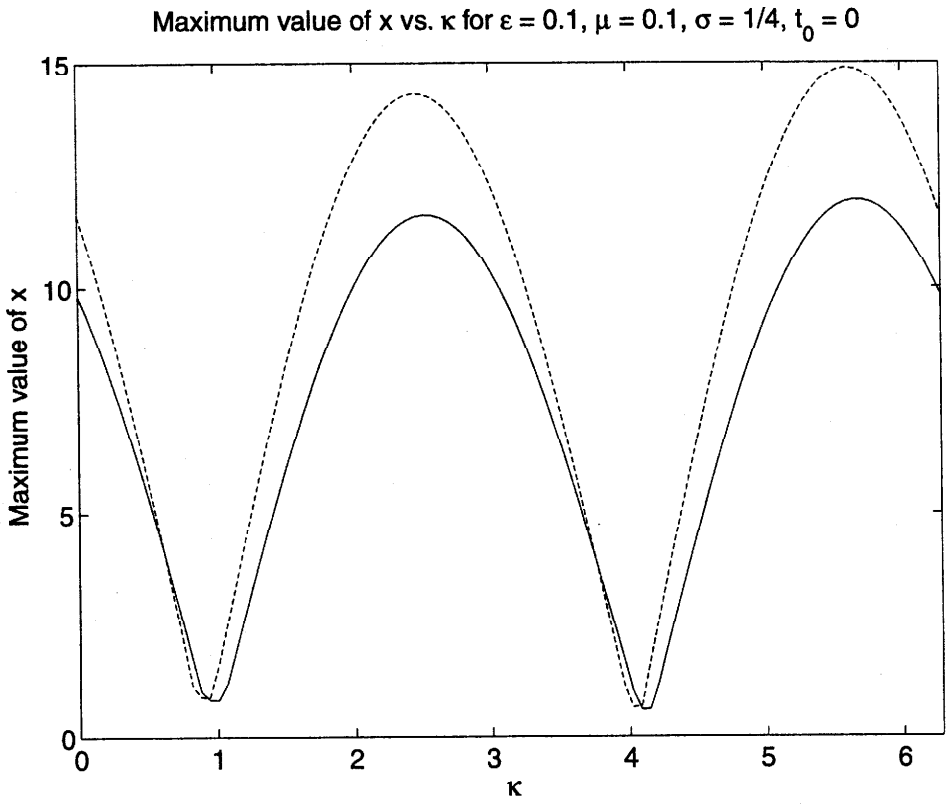

Figure 8. Comparison of the multiple scales approximation with the original equation. The solid line denotes the original equation, and the dashed line denotes the multiple scales approximation. The maximum value of x is shown as a function of the initial condition parameter κ for $t_0 = 0$.

where the prime ($'$) denotes differentiation with respect to τ. For small values of μ, the WKB method can be applied. Application of the WKB method to equation (23) involves the ansatz

$$y \sim \mathrm{e}^{\frac{1}{\mu}\phi(\tau)} \left(y_0(\tau) + \mu y_1(\tau) + \ldots\right). \tag{24}$$

The asymptotic expansions of the first and second derivatives of the solution are

$$y' \sim \mathrm{e}^{\frac{1}{\mu}\phi} \left(\mu^{-1}\phi' y_0 + y_0' + \phi' y_1 + \ldots\right) \tag{25}$$

$$y'' \sim \mathrm{e}^{\frac{1}{\mu}\phi} \left(\mu^{-2}(\phi')^2 y_0 + \mu^{-1}(\phi'' y_0 + 2\phi' y_0' + (\phi')^2 y_1) + \ldots\right). \tag{26}$$

Substituting equations (25) and (26) into equation (23) gives

$$\mu^2 \left(\mu^{-2}(\phi')^2 y_0 + \mu^{-1}(\phi'' y_0 + 2\phi' y_0' + (\phi')^2 y_1) + \ldots\right)$$

$$-q(\tau)\left(y_0+\mu y_1+\ldots\right)+\mu^2 p(\tau)\left(\mu^{-1}\phi' y_0+y_0'+\phi' y_1+\ldots\right) \;=\; 0. \tag{27}$$

Collecting $O(1)$ and $O(\mu)$ terms results in the following equations:

$$O(1) \;:\; (\phi')^2 y_0 - q y_0 = 0 \tag{28}$$

$$O(\mu) \;:\; \phi'' y_0 + 2\phi' y_0' + (\phi')^2 y_1 - q y_1 + p\phi' y_0 = 0. \tag{29}$$

From equation (28) we have

$$(\phi')^2 - q = 0 \Rightarrow \phi' = \pm\sqrt{q} \Rightarrow \phi = \pm\int^{\tau}\sqrt{q(s)}\mathrm{d}s. \tag{30}$$

With $\phi' = \pm\sqrt{q}$ and $\phi'' = \pm\frac{q'}{2\sqrt{q}}$, equation (29) becomes

$$\pm\frac{1}{2\sqrt{q}}q' y_0 \pm 2\sqrt{q} y_0' \pm \sqrt{q} y_0 = 0 \tag{31}$$

which can be rewritten as

$$\frac{y_0'}{y_0} = -\frac{q'}{4q} - \frac{p}{2}. \tag{32}$$

Integrating equation (32) gives

$$\int\frac{y_0'}{y_0} = \int\left(-\frac{q'}{4q}-\frac{p}{2}\right) \Rightarrow \log y_0 = -\frac{1}{4}\log q - \frac{1}{2}\int^{\tau} p(s)\mathrm{d}s. \tag{33}$$

Taking the exponential of both side of equation (33) gives

$$y_0(\tau) = q(\tau)^{-1/4}\exp\left(-\frac{1}{2}\int^{\tau} p(s)\mathrm{d}s\right). \tag{34}$$

Taking equations (24), (30) and (34), the WKB approximation of equation (23) is

$$y(\tau) \sim \frac{\exp\left(-\frac{1}{2}\int^{\tau} p(s)\mathrm{d}s\right)}{q(\tau)^{1/4}}\left[C_1\exp\left(\frac{1}{\mu}\int^{\tau}\sqrt{q(s)}\mathrm{d}s\right) + C_2\exp\left(-\frac{1}{\mu}\int^{\tau}\sqrt{q(s)}\mathrm{d}s\right)\right]. \tag{35}$$

The system has a turning point at $\tau = \tau^*$ if $q(\tau^*) = 0$. If $q(\tau) < 0$ for $\tau < \tau^*$ and $q(\tau) > 0$ for $\tau > \tau^*$ then equation (35) can be written as

$$y_L(\tau) \sim \frac{\exp\left(-\frac{1}{2}\int^{\tau} p(s)\mathrm{d}s\right)}{(-q)^{1/4}}\left[C_{L1}\cos\left(\frac{\phi_L}{\mu}+\frac{\pi}{4}\right) + C_{L2}\cos\left(\frac{\phi_L}{\mu}-\frac{\pi}{4}\right)\right], \quad \tau < \tau^* \tag{36}$$

$$y_R(\tau) \sim \frac{\exp\left(-\frac{1}{2}\int^{\tau} p(s)\mathrm{d}s\right)}{q^{1/4}}\left[C_{R1}\,\mathrm{e}^{\frac{\phi_R}{\mu}} + C_{R2}\,\mathrm{e}^{-\frac{\phi_R}{\mu}}\right], \quad \tau > \tau^* \tag{37}$$

where

$$\phi_L = \int_{\tau}^{\tau^*} \sqrt{-q(s)}\mathrm{d}s, \qquad \phi_R = \int_{\tau^*}^{\tau} \sqrt{q(s)}\mathrm{d}s.$$

The approximation near the turning point depends on the form of $q(\tau)$ and $p(\tau)$. For $q'(\tau^*) \neq 0$ and $p(\tau^*) \sim$ const, the solution takes the form of Airy functions. Detailed calculations will be shown for specific choices of $q(\tau)$ and $p(\tau)$. A relation between the constants C_{L1} and C_{L2}, which occur in the $\tau < \tau^*$ solution (equation (36)), and C_{R1} and C_{R2}, which occur in the $\tau > \tau^*$ solution (equation (37)), are found by matching with another approximation, which is valid at the turning point.

Similarly, if $q(\tau) > 0$ for $\tau < \tau^*$ and $q(\tau) < 0$ for $\tau > \tau^*$, equation (35) can be written as

$$y_L(\tau) \sim \frac{\exp\left(-\frac{1}{2}\int^{\tau} p(s)\mathrm{d}s\right)}{q^{-1/4}}\left[C_{L1}\,\mathrm{e}^{\frac{\phi_L}{\mu}} + C_{L2}\,\mathrm{e}^{-\frac{\phi_L}{\mu}}\right], \ \tau < \tau^* \tag{38}$$

$$y_R(\tau) \sim \frac{\exp\left(-\frac{1}{2}\int^{\tau} p(s)\mathrm{d}s\right)}{(-q)^{-1/4}}\left[C_{R1}\cos\left(\frac{\phi_R}{\mu} + \frac{\pi}{4}\right) + C_{R2}\cos\left(\frac{\phi_R}{\mu} - \frac{\pi}{4}\right)\right], \ \tau > \tau^* \tag{39}$$

where

$$\phi_L = \int_{\tau}^{\tau^*} \sqrt{q(s)}\mathrm{d}s, \qquad \phi_R = \int_{\tau^*}^{\tau} \sqrt{-q(s)}\mathrm{d}s.$$

4.2. Application to the Slow Flow

We apply the WKB method to the equation on A (equation (17)) obtained from the slow flow equations. In equation (17), $q = 1/4 - \tau^2$ so we have turning points at $\tau = \pm 1/2$. Because we have two turning points, the approximation can be divided into five different regions:

- A_1 in the region $\tau < -1/2$, before turning points;
- A_2 in the region $\tau \approx -1/2$, near turning point at $\tau = -1/2$;
- A_3 in the region $-1/2 < \tau < 1/2$, between the two turning points;
- A_4 in the region $\tau \approx 1/2$, near turning point at $\tau = 1/2$;
- A_5 in the region $\tau > 1/2$, after turning points.

Also in equation (17) we have $p = \frac{-1}{\tau - 1/2}$, so solving for the exponential in the y_0 term in equation (34) gives

$$\exp\left(-\frac{1}{2}\int^{\tau} p(s)\mathrm{d}s\right) = \exp\left(\frac{1}{2}\int^{\tau} \frac{1}{s-1/2}\mathrm{d}s\right) = \exp\left(\frac{1}{2}\log|\tau-1/2|\right) = \sqrt{|\tau-\frac{1}{2}|}. \tag{40}$$

We begin by finding A_1, an expression for A valid for $\tau < -1/2$, and A_3, an expression for A valid for $-1/2 < \tau < 1/2$. For $\tau < -1/2$, $q(\tau) > 0$ and for $-1/2 < \tau < 1/2$, $q(\tau) < 0$ so the approximation is of the form of equations (36) and (37). Thus, the WKB approximations for A_1 and A_3 are

$$A_1 = \frac{\left(\frac{1}{2}-\tau\right)^{1/2}}{\left(\tau^2-\frac{1}{4}\right)^{1/4}}\left[C_{11}\cos\left(\frac{\phi_1}{\mu}+\frac{\pi}{4}\right)+C_{12}\cos\left(\frac{\phi_1}{\mu}-\frac{\pi}{4}\right)\right],\ \tau < -\frac{1}{2} \tag{41}$$

$$A_3 = \frac{\left(\frac{1}{2}-\tau\right)^{1/2}}{\left(\frac{1}{4}-\tau^2\right)^{1/4}}\left(C_{31}\,\mathrm{e}^{\frac{1}{\mu}\phi_3}+C_{32}\,\mathrm{e}^{-\frac{1}{\mu}\phi_3}\right),\ -\frac{1}{2} < \tau < \frac{1}{2} \tag{42}$$

where

$$\phi_1 = \int_{\tau}^{-1/2}\sqrt{s^2-\frac{1}{4}}\mathrm{d}s = -\frac{2\tau\sqrt{4\tau^2-1}-\log\left(-\sqrt{4\tau^2-1}-2\tau\right)}{8}$$

$$\phi_3 = \int_{-1/2}^{\tau}\sqrt{\frac{1}{4}-s^2}\mathrm{d}s = \frac{\arcsin(2\tau)+2\tau\sqrt{1-4\tau^2}}{8}+\frac{\pi}{16}.$$

To obtain an approximation near the turning point at $\tau = -1/2$, we make the change of variables $z = \frac{\tau+1/2}{\mu^\beta}$. Near the turning point, equation (17) behaves like

$$\mu^{2-2\beta}A'' - z\mu^\beta A - \mu^{2-\beta}A' = 0. \tag{43}$$

Choosing $\beta = 2/3$ balances the A'' and A terms which gives the equation

$$A'' - zA = 0 \tag{44}$$

which is just the Airy equation. The solution can be written in terms of Airy functions:

$$A_2 = C_{21}Ai(z) + C_{22}Bi(z) = C_{21}Ai\left(\frac{\tau+\frac{1}{2}}{\mu^{2/3}}\right) + C_{22}Bi\left(\frac{\tau+\frac{1}{2}}{\mu^{2/3}}\right). \tag{45}$$

Equations (41), (42) and (45) now form the WKB approximation. The six constants (C) can be reduced to two by matching the solutions. To match the solutions, we use asymptotic expansions of the approximations; see Appendix A for details of the matching procedure. We find the following equations relating C_{21}, C_{22}, C_{31}, C_{32} to C_{11}, C_{12}:

$$C_{31} = C_{11}, \qquad C_{32} = \frac{C_{12}}{2}, \qquad C_{21} = \sqrt{\pi}\mu^{-1/6}C_{12}, \qquad C_{22} = \sqrt{\pi}\mu^{-1/6}C_{11}. \quad (46)$$

Our WKB approximations of A using equation (17) are

$$A_1 = \frac{\left(\frac{1}{2}-\tau\right)^{1/2}}{\left(\tau^2-\frac{1}{4}\right)^{1/4}}\left[C_{11}\cos\left(\frac{\phi_1}{\mu}+\frac{\pi}{4}\right)+C_{12}\cos\left(\frac{\phi_1}{\mu}-\frac{\pi}{4}\right)\right], \quad \tau < -\frac{1}{2} \quad (47)$$

$$A_2 = \frac{\sqrt{\pi}}{\mu^{1/6}}\left[C_{12}Ai\left(\frac{\tau+\frac{1}{2}}{\mu^{2/3}}\right)+C_{11}Bi\left(\frac{\tau+\frac{1}{2}}{\mu^{2/3}}\right)\right], \quad \tau \approx -\frac{1}{2} \quad (48)$$

$$A_3 = \frac{\left(\frac{1}{2}-\tau\right)^{1/2}}{\left(\frac{1}{4}-\tau^2\right)^{1/4}}\left(C_{11}\,\mathrm{e}^{\frac{1}{\mu}\phi_3}+\frac{C_{12}}{2}\,\mathrm{e}^{-\frac{1}{\mu}\phi_3}\right), \quad -\frac{1}{2} < \tau < \frac{1}{2} \quad (49)$$

where

$$\phi_1 = -\frac{2\tau\sqrt{4\tau^2-1}-\log\left(-\sqrt{4\tau^2-1}-2\tau\right)}{8}$$

$$\phi_3 = \frac{\arcsin(2\tau)+2\tau\sqrt{1-4\tau^2}}{8}+\frac{\pi}{16}.$$

So far, we have used the WKB method on the A equation (equation (17)). Since equation (17) is singular at $\tau = 1/2$, we now switch to the B equation (equation (18)) to study the behavior in the neighborhood of $\tau = 1/2$. In a similar fashion as before, we obtain

$$B_3 = \frac{\left(\tau+\frac{1}{2}\right)^{1/2}}{\left(\frac{1}{4}-\tau^2\right)^{1/4}}\left(D_{31}\,\mathrm{e}^{\frac{1}{\mu}\phi_3^*}+D_{32}\,\mathrm{e}^{-\frac{1}{\mu}\phi_3^*}\right), \quad -\frac{1}{2} < \tau < \frac{1}{2} \quad (50)$$

$$B_4 = \frac{\sqrt{\pi}}{\mu^{1/6}}\left[2D_{32}Ai\left(\frac{\frac{1}{2}-\tau}{\mu^{2/3}}\right)+D_{31}Bi\left(\frac{\frac{1}{2}-\tau}{\mu^{2/3}}\right)\right], \quad \tau \approx \frac{1}{2} \quad (51)$$

$$B_5 = \frac{\left(\tau+\frac{1}{2}\right)^{1/2}}{\left(\tau^2-\frac{1}{4}\right)^{1/4}}\left[D_{31}\cos\left(\frac{\phi_5}{\mu}+\frac{\pi}{4}\right)+2D_{32}\cos\left(\frac{\phi_5}{\mu}-\frac{\pi}{4}\right)\right], \quad \tau > \frac{1}{2} \quad (52)$$

where

$$\phi_3^* = \frac{\pi}{16}-\frac{\arcsin(2\tau)+2\tau\sqrt{1-4\tau^2}}{8} = -\phi_3+\frac{\pi}{8}$$

$$\phi_5 = \frac{2\tau\sqrt{4\tau^2-1}-\log\left(\sqrt{4\tau^2-1}+2\tau\right)}{8}.$$

The approximation for B can then be used to give an approximation for A around $\tau = 1/2$ by taking the derivative of equations (50)–(52) and using equation (14) which relates A to $dB/d\eta$ (or $dB/d\tau$). This avoids analyzing equation (17) around $\tau = 1/2$ where it is singular. Doing this we obtain

$$A_3^* = -\frac{D_{31}(2\mu - (1-4\tau^2)^{3/2})e^{\frac{1}{\mu}\phi_3^*} + D_{32}(2\mu + (1-4\tau^2)^{3/2})e^{-\frac{1}{\mu}\phi_3^*}}{\sqrt{2\tau+1}(1-4\tau^2)^{5/4}} \tag{53}$$

$$A_4 = \frac{2\mu^{1/3}\sqrt{\pi}}{2\tau+1}\left[2D_{32}Ai'\left(\frac{\frac{1}{2}-\tau}{\mu^{2/3}}\right) + D_{31}Bi'\left(\frac{\frac{1}{2}-\tau}{\mu^{2/3}}\right)\right] \tag{54}$$

$$A_5 = \left[(2D_{31}\mu - 2D_{32}(4\tau^2-1)^{3/2})\cos\left(\frac{\phi_5}{\mu}+\frac{\pi}{4}\right)\right.$$
$$\left. + (4D_{32}\mu + D_{31}(4\tau^2-1)^{3/2})\cos\left(\frac{\phi_5}{\mu}-\frac{\pi}{4}\right)\right] / \left[\sqrt{2\tau+1}(4\tau^2-1)^{5/4}\right] \tag{55}$$

where

$$\phi_3^* = \frac{\pi}{16} - \frac{\arcsin 2\tau + 2\tau\sqrt{1-4\tau^2}}{8}$$
$$\phi_5 = \frac{2\tau\sqrt{4\tau^2-1} - \log(\sqrt{4\tau^2-1}+2\tau)}{8}.$$

We have two approximations for A in the region between the two turning points: A_3 (from applying the WKB method to equation (17)) and A_3^* (from applying the WKB method to equation (18) and then using equation (14)). To combine the two approximations, we take A_3 for $\tau \leq 0$ and A_3^* for $\tau \geq 0$ and we match A_3 to A_3^* and their derivatives at $\tau = 0$ requiring

$$A_3(0) = A_3^*(0) \qquad \text{and} \qquad \frac{dA_3}{d\tau}(0) = \frac{dA_3^*}{d\tau}(0). \tag{56}$$

Doing this, we obtain the following relations between D_{31}, D_{32} and C_{11}, C_{12}:

$$D_{31} = -\frac{C_{12}}{2(2\mu-1)}e^{-\frac{\pi}{8\mu}} \tag{57}$$

$$D_{32} = -\frac{C_{11}}{2\mu+1}e^{\frac{\pi}{8\mu}}. \tag{58}$$

Finally we must be able to solve for C_{11}, C_{12} in terms of the initial conditions $A(\tau_0)$, $B(\tau_0)$. Let us assume that our initial conditions are prescribed for $\tau_0 < -1/2$ (i.e. before the motion enters the resonance tongue) so $A(\tau_0) = A_1(\tau_0)$. We can obtain $B(\tau_0)$ from $A_1(\tau_0)$ using equation (13). The equations relating $A(\tau_0)$, $B(\tau_0)$ to C_{11}, C_{12} are

$$A(\tau_0) = A_1(\tau_0) = K_{11}(\tau_0)C_{11} + K_{12}(\tau_0)C_{12} \tag{59}$$

$$B(\tau_0) = \frac{\mu}{\tau_0 - \frac{1}{2}} \frac{\mathrm{d}A_1}{\mathrm{d}\tau}(\tau_0) = K_{21}(\tau_0)C_{11} + K_{22}(\tau_0)C_{12}. \tag{60}$$

See Appendix B for the expressions for $K_{ij}(\tau_0)$. Equations (59) and (60) can be expressed in matrix form:

$$\begin{bmatrix} A(\tau_0) \\ B(\tau_0) \end{bmatrix} = \begin{bmatrix} K_{11}(\tau_0) & K_{12}(\tau_0) \\ K_{21}(\tau_0) & K_{22}(\tau_0) \end{bmatrix} \begin{bmatrix} C_{11} \\ C_{12} \end{bmatrix}. \tag{61}$$

We can find C_{11}, C_{12} in terms of $A(\tau_0)$, $B(\tau_0)$ using the inverse of the $K_{ij}(\tau_0)$ matrix

$$\begin{bmatrix} C_{11} \\ C_{12} \end{bmatrix} = \begin{bmatrix} K_{11}(\tau_0) & K_{12}(\tau_0) \\ K_{21}(\tau_0) & K_{22}(\tau_0) \end{bmatrix}^{-1} \begin{bmatrix} A(\tau_0) \\ B(\tau_0) \end{bmatrix}. \tag{62}$$

Finally, our WKB approximation of A is given by equations (47)–(49), (53)–(55), and (57), (58). The constants C_{11}, C_{12} are related to the initial conditions $A(\tau_0)$, $B(\tau_0)$ by equation (62). An expression for B can be obtained using the A approximation and equation (13).

Figure 9 shows a comparison of the WKB approximation with numerical integration of the slow flow equations for $\mu = 0.1$, $\tau_0 = -2.5$ and the initial conditions $A(\tau_0) = 1$, $B(\tau_0) = 0$. Figure 10 shows a close up of Figure 9 for the region around the first turning point. The approximation is nearly indistinguishable from the numerical integration prior to the second turning point. Around the second turning point, the error becomes more significant and the amplitude is smaller in the approximation. However, the phase is well approximated throughout the solution.

Recall that the multiple scales approximation becomes worse as we get farther away from the 2:1 resonance ($|t|$ becomes larger); see Figure 6. Because the WKB approximation is based on the slow flow equations, it also is only good for values of $|t|$ (or $|\eta|$ and $|\tau|$) that are not too large.

5. AMPLIFICATION IN THE RESONANCE REGION

The performed WKB analysis can help us to understand the phenomena of amplification (or de-amplification) in the resonance region. The turning points in our WKB analysis correspond to the transition curves of the resonance region. At the turning points, the nature of the solution changes from oscillatory to exponential. Outside the resonance region, the WKB approximation has oscillatory solutions so amplification does not occur. Inside the resonance region, the WKB approximation has exponentially growing and decaying solutions which can result in amplification (or de-amplification).

The WKB approximation can be used to determine which initial conditions result in the smallest oscillation amplitude after passing through the resonance tongue. The initial conditions should be chosen so that the WKB approximation between the turning points (A_3), i.e. inside the resonant tongue, does not have an exponentially growing component. This requires the constant $C_{11} = 0$ (see equation (49)). The initial conditions leading to maximum de-amplification can be found using equation (61)

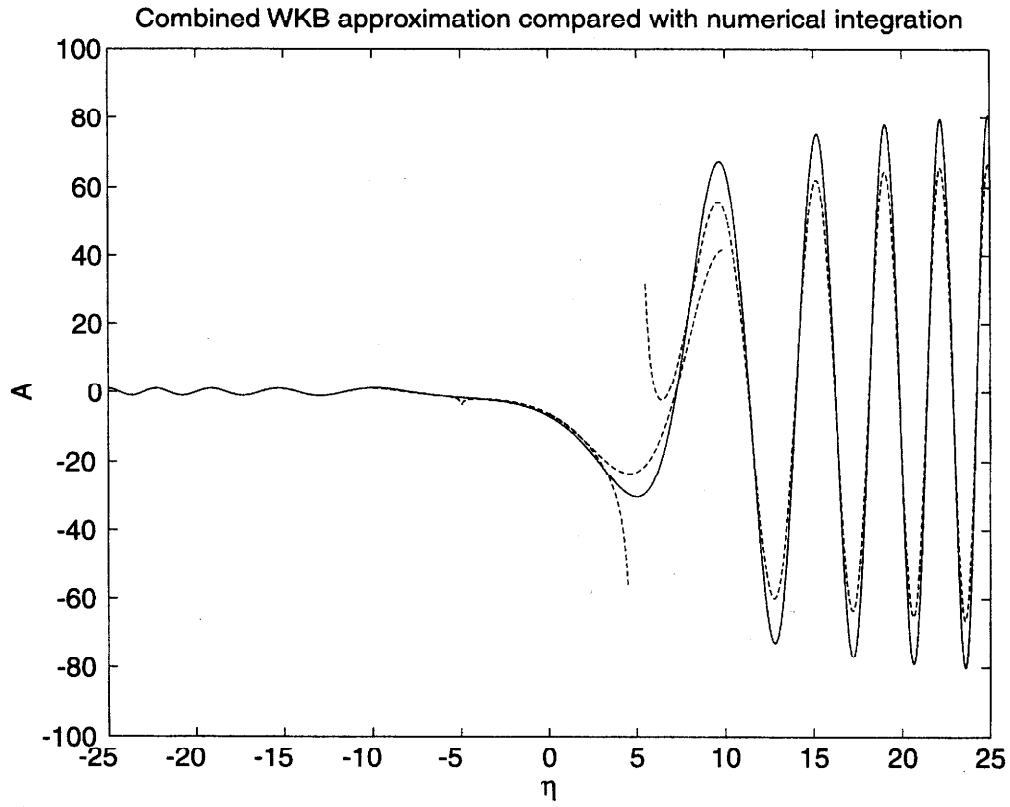

Figure 9. Comparison of the WKB approximation with the numerical integration of slow flow. The solid line denotes numerical integration, the dashed lines are WKB approximations away from turning points (A_1, A_3, A_3^*, A_5) and the dashed-dotted lines are WKB approximations at turning points (A_2, A_4). The parameters are $\mu = 0.1$, $\tau_0 = -2.5$, $\eta_0 = -25$ and the initial conditions are $A(\tau_0) = 1$, $B(\tau_0) = 0$.

$$\begin{bmatrix} A(\tau_0) \\ B(\tau_0) \end{bmatrix} = \begin{bmatrix} K_{11}(\tau_0) & K_{12}(\tau_0) \\ K_{21}(\tau_0) & K_{22}(\tau_0) \end{bmatrix} \begin{bmatrix} 0 \\ C_{12} \end{bmatrix} \tag{63}$$

which gives

$$A(\tau_0) = K_{12}(\tau_0)C_{12}, \qquad B(\tau_0) = K_{22}(\tau_0)C_{12}. \tag{64}$$

If we again assume initial conditions of the form of equations (22), we can solve for the value of κ which gives the maximum de-amplification:

$$\tan \kappa_{min} = \frac{B(\tau_0)}{A(\tau_0)} = \frac{K_{22}(\tau_0)}{K_{12}(\tau_0)} \quad \Rightarrow \quad \kappa_{min} = \arctan\left(\frac{K_{22}(\tau_0)}{K_{12}(\tau_0)}\right). \tag{65}$$

Using the expressions for $K_{12}(\tau_0)$ and $K_{22}(\tau_0)$ in Appendix B, we obtain

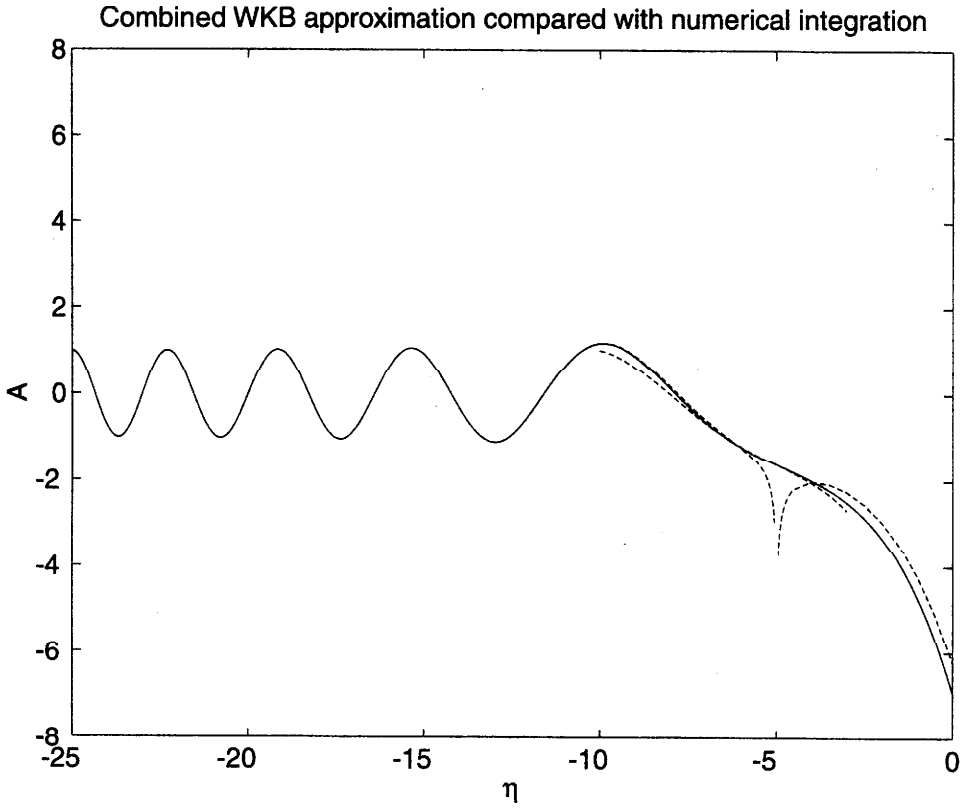

Figure 10. Comparison of the WKB approximation with the numerical integration of slow flow. This figure is an enlargement of Figure 9. The solid line denotes the numerical integration, the dashed lines are WKB approximations away from turning points (A_1, A_3) and the dashed-dotted line is the WKB approximation at turning point (A_2). The parameters are $\mu = 0.1$, $\tau_0 = -2.5$, $\eta_0 = -25$ and the initial conditions are $A(\tau_0) = 1$, $B(\tau_0) = 0$.

$$\kappa_{min} = \arctan\left(\frac{(4\tau_0^2-1)^{3/2}\cos\left(\frac{\phi_1(\tau_0)}{\mu}+\frac{\pi}{4}\right) - 2\mu\cos\left(\frac{\phi_1(\tau_0)}{\mu}-\frac{\pi}{4}\right)}{(1-2\tau_0)(4\tau_0^2-1)\cos\left(\frac{\phi_1(\tau_0)}{\mu}-\frac{\pi}{4}\right)}\right) \tag{66}$$

where $\phi_1(\tau_0)$ is given by equation (78) in Appendix B.

We can also obtain an expression for $\kappa_{\max}$ where the maximum amplification occurs by taking $C_{12} = 0$ instead of C_{11} and repeating the calculation above.

For $\mu = 0.1$, $\tau_0 = -1$, using equation (66) we obtain $\kappa_{\min} = 1.0328$. Numerical integration of the slow flow equations shows that maximum de-amplification occurs when $\kappa \approx 1.1123$, which is close to the value predicted by the WKB method. For $\epsilon = 0.1$, numerical integration of the original equation, for this case in which $\mu = 0.1$, $\tau_0 = -1$, $t_0 = -100$, shows that maximum de-amplification occurs when $\kappa \approx 0.9304$, which is again close to the value predicted by the WKB method (see Figure 7).

6. CONCLUSIONS

We have found that amplification/de-amplification can occur for slow passage through resonance in Mathieu's equation. The degree of amplification depends on the initial conditions. A very small range of initial conditions can lead to de-amplification.

Using the method of multiple scales, we have obtained a system of slow flow equations which approximates equation (3) around the 2:1 resonance. The WKB method was applied to the slow flow equations. Turning points in the WKB approximation correspond to the transition curves of the linear Mathieu equation. Outside of the resonance tongue, the WKB approximation has oscillatory solutions; inside the tongue, the WKB approximation has exponentially growing and decaying solutions. By choosing the constants of the WKB approximation such that there is only a decaying solution in the resonance region, we can obtain an approximation for the initial conditions in the slow flow, which result in the smallest amplitude after passing through the tongue.

In the WKB analysis, we found that around the turning points there is a boundary layer of thickness $\mu^{2/3}$ where the solution changes from oscillatory to exponential. Thus, as the value μ increases, so does the thickness of the boundary layer. The turning points of the system are located at $\tau = \pm 1/2$. As the boundary layers become thicker, the region of exponential growth between the turning points becomes smaller. When $\mu = 2^{-3/2} \approx 0.35355$, the boundary layers from the two turning points meet. For values of $\mu \geq 2^{-3/2}$, the boundary layers overlap and the region of exponential-type solutions disappears. Thus, we would expect for $\mu \geq 2^{-3/2}$ that the solutions do not exhibit the amplification/de-amplification associated with the region where exponential solutions exist. Of course, the WKB method is only valid for small values of μ but this criterion could be viewed as a heuristic for the case when the resonant effects going through the tongue are no longer significant. Numerical integration shows that generally, when μ is near the value predicted, the amount of amplification/de-amplication is not as significant. However, this is difficult to quantify because, as seen previously, the amount of amplification/de-amplification depends on the initial conditions.

APPENDIX A

Matching different parts of the WKB approximation requires the use of their asymptotic expansions. The asymptotic expansions of equation (48) are

$$A_2 \sim \frac{z^{-1/4}}{2\sqrt{\pi}} \left[C_{21} \mathrm{e}^{-\frac{2}{3}z^{3/2}} + 2C_{22} \mathrm{e}^{\frac{2}{3}z^{3/2}} \right], \quad z \to \infty \tag{67}$$

$$A_2 \sim \frac{|z|^{-1/4}}{\sqrt{\pi}} \left[C_{21} \cos\left(\frac{2}{3}|z|^{3/2} - \frac{\pi}{4} \right) + C_{22} \cos\left(\frac{2}{3}|z|^{3/2} + \frac{\pi}{4} \right) \right], \quad z \to -\infty \tag{68}$$

where $z = \frac{\tau + \frac{1}{2}}{\mu^{2/3}}$.

The asymptotic expansions of equations (47) and (49) are

$$A_1 \sim \frac{|z|^{-1/4}}{\mu^{1/6}}\left(C_{11}\cos\left(\frac{2}{3}|z|^{3/2}+\frac{\pi}{4}\right)+C_{12}\cos\left(\frac{2}{3}|z|^{3/2}-\frac{\pi}{4}\right)\right),\ \tau\to-\frac{1}{2} \quad (69)$$

$$A_3 \sim \frac{z^{-1/4}}{\mu^{1/6}}\left(C_{31}e^{\frac{2}{3}z^{3/2}}+C_{32}e^{-\frac{2}{3}z^{3/2}}\right),\ \tau\to-\frac{1}{2}. \quad (70)$$

Equating the coefficients in equation (67) to equation (70), and those in equation (68) to equation (69), gives the following equations relating C_{21}, C_{22}, C_{31}, C_{32} to C_{11}, C_{12}:

$$C_{21}=\sqrt{\pi}\mu^{-1/6}C_{12},\quad C_{22}=\sqrt{\pi}\mu^{-1/6}C_{11},\quad C_{31}=C_{11},\quad C_{32}=\frac{C_{12}}{2}. \quad (71)$$

The asymptotic expansions of equation (51) are

$$B_4 \sim \frac{z^{-1/4}}{\sqrt{\pi}}\left[D_{41}\cos\left(\frac{2}{3}z^{3/2}-\frac{\pi}{4}\right)+D_{42}\cos\left(\frac{2}{3}z^{3/2}+\frac{\pi}{4}\right)\right],\quad z\to\infty \quad (72)$$

$$B_4 \sim \frac{|z|^{-1/4}}{2\sqrt{\pi}}\left[D_{41}e^{-\frac{2}{3}|z|^{3/2}}+2D_{42}e^{\frac{2}{3}|z|^{3/2}}\right],\quad z\to-\infty \quad (73)$$

where $z=\frac{\tau-\frac{1}{2}}{\mu^{2/3}}$.

The asymptotic expansions of equations (50) and (52) are

$$B_3 \sim \frac{|z|^{-1/4}}{\mu^{1/6}}\left[D_{31}e^{\frac{2}{3}|z|^{3/2}}+D_{32}e^{-\frac{2}{3}|z|^{3/2}}\right],\quad \tau\to\frac{1}{2} \quad (74)$$

$$B_5 \sim \frac{z^{-1/4}}{\mu^{1/6}}\left[D_{51}\cos\left(\frac{2}{3}z^{3/2}+\frac{\pi}{4}\right)+D_{52}\cos\left(\frac{2}{3}z^{3/2}-\frac{\pi}{4}\right)\right],\quad \tau\to\frac{1}{2}. \quad (75)$$

Equating the coefficients in equation (72) to equation (75), and those in equation (73) to equation (74), gives the following equations relating D_{41}, D_{42}, D_{51}, D_{52} to D_{31}, D_{32}:

$$D_{41}=2\sqrt{\pi}\mu^{-1/6}D_{32},\quad D_{42}=\sqrt{\pi}\mu^{-1/6}D_{31},\quad D_{51}=D_{31},\quad D_{52}=2D_{32}. \quad (76)$$

APPENDIX B

Expressions are given for $K_{ij}(\tau_0)$ which relate initial conditions of the slow flow equations $(A(\tau_0), B(\tau_0))$ to the constants in the WKB approximation (C_{11}, C_{12}). From equation (59) we have

$$A(\tau_0) = A_1(\tau_0) = K_{11}(\tau_0)C_{11} + K_{12}(\tau_0)C_{12}$$
$$= \frac{\left(\frac{1}{2} - \tau_0\right)^{1/2}}{\left(\tau_0^2 - \frac{1}{4}\right)^{1/4}} \left[C_{11}\cos\left(\frac{\phi_1(\tau_0)}{\mu} + \frac{\pi}{4}\right) + C_{12}\cos\left(\frac{\phi_1(\tau_0)}{\mu} - \frac{\pi}{4}\right)\right] \quad (77)$$

where

$$\phi_1(\tau_0) = -\frac{2\tau_0\sqrt{4\tau_0^2 - 1} - \log\left(-\sqrt{4\tau_0^2 - 1} - 2\tau_0\right)}{8}. \quad (78)$$

Collecting terms in equation (77), we obtain

$$K_{11}(\tau_0) = \frac{\left(\frac{1}{2} - \tau_0\right)^{1/2}}{\left(\tau_0^2 - \frac{1}{4}\right)^{1/4}} \cos\left(\frac{\phi_1(\tau_0)}{\mu} + \frac{\pi}{4}\right) \quad (79)$$

$$K_{12}(\tau_0) = \frac{\left(\frac{1}{2} - \tau_0\right)^{1/2}}{\left(\tau_0^2 - \frac{1}{4}\right)^{1/4}} \cos\left(\frac{\phi_1(\tau_0)}{\mu} - \frac{\pi}{4}\right). \quad (80)$$

From equation (60) we have

$$B(\tau_0) = \frac{\mu}{\tau_0 - \frac{1}{2}} \frac{dA_1}{d\tau}(\tau_0) = K_{21}(\tau_0)C_{11} + K_{22}(\tau_0)C_{12}$$
$$= -\left[\left(2C_{11}\mu - C_{12}(4\tau_0^2 - 1)^{3/2}\right)\cos\left(\frac{\phi_1(\tau_0)}{\mu} + \frac{\pi}{4}\right)\right.$$
$$+ \left.\left(2C_{12}\mu + C_{11}(4\tau_0^2 - 1)^{3/2}\right)\cos\left(\frac{\phi_1(\tau_0)}{\mu} - \frac{\pi}{4}\right)\right] /$$
$$\left[\sqrt{1 - 2\tau_0}(4\tau_0^2 - 1)^{5/4}\right]. \quad (81)$$

Collecting terms in equation (81), we obtain

$$K_{21}(\tau_0) = -\left[2\mu\cos\left(\frac{\phi_1(\tau_0)}{\mu} + \frac{\pi}{4}\right) + (4\tau_0^2 - 1)^{3/2}\cos\left(\frac{\phi_1(\tau_0)}{\mu} - \frac{\pi}{4}\right)\right] /$$
$$\left[\sqrt{1 - 2\tau_0}(4\tau_0^2 - 1)^{5/4}\right] \quad (82)$$

$$K_{22}(\tau_0) = \left[(4\tau_0^2 - 1)^{3/2}\cos\left(\frac{\phi_1(\tau_0)}{\mu} + \frac{\pi}{4}\right) - 2\mu\cos\left(\frac{\phi_1(\tau_0)}{\mu} - \frac{\pi}{4}\right)\right] /$$
$$\left[\sqrt{1 - 2\tau_0}(4\tau_0^2 - 1)^{5/4}\right]. \quad (83)$$

Acknowledgments. This work was partially supported by the Natural Sciences and Engineering Research Council of Canada (NSERC), the Office of Naval Research, Program Officer Dr. Roy Elswick, Code 321 and the National Space Grant College and Fellowship Program, NASA/NY Space Grant Consortium under Grant No NGT5-40078.

REFERENCES

Bender, C.M. and Orszag, S.A., 1999, *Advanced Mathematical Methods for Scientists and Engineers*, Springer-Verlag, New York.

Holmes, M.H., 1995, *Introduction to Perturbation Methods*, Springer-Verlag, New York.

Levobitz, N.R. and Pesci, A.I., 1995, "Dynamic bifurcation in hamiltonian systems with one degree of freedom," *SIAM Journal of Applied Mathematics* **55**(4), 1117–1133.

Nayfeh, A.H. and Asfar, K.R., 1988, "Non-stationary parametric oscillations," *Journal of Sound and Vibration* **124**(3), 529–537.

Neal, H.L. and Nayfeh, A.H., 1990, "Response of a single-degree-of-freedom system to a non-stationary principal parametric excitation," *International Journal of Non-Linear Mechanics* **25**(2/3), 275–284.

Raman, A., Bajaj, A.K., and Davies, P., 1996, "On the slow transition across instabilities in non-linear dissipative systems," *Journal of Sound and Vibration* **192**(4), 835–865.

Raman, A. and Bajaj, A.K., 1998, "On the non-stationary passage through bifurcations in resonantly forced Hamiltonian oscillators," *International Journal of Non-Linear Mechanics* **33**(5), 907–933.

Stoker, J.J., 1950, *Nonlinear Vibrations in Mechanical and Electrical Systems*, Wiley, New York.